Distribution of Supernova Remnants

Masaki Mori

References:

Case & Battacharya, *Astrophys. J.* 504:761, 1998
Urosevic et al., *Astron.Astrophys.* 435, 437, 2005
Brogan et al., *astro-ph/0601451*

ICRR CANGAROO group internal seminar, March 6, 2006

Case & Battacharya, ApJ 504, 761, 1998

Observation of SNRs

- Radio SNR survey: selection biases
  - Overlook low-surface-brightness SNRs
  - Overlook small-angular-size SNRs
  - Absence of uniform coverage of sky
- Distances to SNRs
  - Positional coincidences with HI, HII and molecular clouds, OB associations, or pulsars or from measuring optical velocities and proper motions

Σ-D relation for SNRs

Clark & Caswell 1976,…

- $\Sigma_\nu = AD^{-\beta}$

$$\Rightarrow d \propto \Sigma_\nu^{1/\beta}\theta^{-1} \propto S_\nu^{1/\beta}\theta^{-(1+2/\beta)}$$

- Σ_ν: radio surface brightness (W $m^{-2}Hz^{-1}sr^{-1}$) Instrinsic property of SNR (Shklovsky 1960)
- D: diameter (pc)
- S_ν: flux density
- θ: angular diameter, $S_\nu \propto \Sigma_\nu\theta^2$

Urosevic, PASRB 4, 113, 2005

Theoretical Σ-D relation (1)

The synchrotron emission power (emissivity) ϵ_ν of this ensemble from a unit volume at a given frequency ν may be expressed as

$$\varepsilon_\nu \propto K H^{1+\alpha} \nu^{-\alpha}, \tag{2}$$

where spectral index $\alpha = (\gamma - 1)/2$. The definition of the spectral index is through $S_\nu \propto \nu^{-\alpha}$, where S_ν is the flux density. The synchrotron surface brightness Σ_ν for an ensemble of relativistic electrons and positrons may be expressed as

$$\Sigma_\nu = \frac{S_\nu}{\Omega} = \frac{\varepsilon_\nu V}{D^2 \pi^2} \propto D K H^{1+\alpha} \nu^{-\alpha}, \tag{3}$$

where Ω is the solid angle, D is the diameter of the spherical volume V of the ensemble with a constant volume emissivity ε_ν and ν is the frequency.

Assuming a constant value for γ, after short derivation (Shklovsky, 1960a), we obtain

$$K = K_0 \left(\frac{D_0}{D}\right)^{\gamma-1} \left(\frac{D_0}{D}\right)^3. \tag{4}$$

Here, K represents the time-evolved value of K_0 as the SNR expands. A major assumption in the derivation presented by Shklovsky (1960a) was that as the spherical nebula (here, an SNR) expands, the structure of the magnetic field is approximately conserved. Therefore, the magnetic field flux must remain constant and H will have the following dependence on radius D:

$$H = H_0 \left(\frac{D_0}{D}\right)^2. \tag{5}$$

Combining the relations given above, we may express the dependence of surface brightness Σ_ν on radius D as

$$\Sigma_\nu \propto D^{-4\alpha-4}. \tag{6}$$

Alternatively, we can express Σ_ν as a function of D as

$$\Sigma_\nu = A D^{-\beta}, \tag{7}$$

where A is a constant and $\beta = 4\alpha + 4$.

Theoretical Σ-D relation (2)

- Shklovsky (1960)
  $\Sigma_\nu = AD^{-6}$
- Lequeux (1962)
  $\Sigma_\nu = AD^{-5.8}$
- Poveda & Woltjer (1968)
  $\Sigma_\nu = AD^{-3}$
- Kesteven (1968)
  $\Sigma_\nu = AD^{-4.5}$
- Duric & Seaquist (1986)
  $\Sigma_\nu = AD^{-2.75\sim3.5}$
- Urosevic (2005)
  $\Sigma_\nu = AD^{-2}$ (evolved) / $AD^{-3.5}$ (young)

Case & Battacharya, ApJ 504, 761, 1998

SHELL SNRs WITH KNOWN DISTANCES

Catalog Name	Other Name	Surface Brightness ($W\ m^{-2}\ Hz^{-1}\ sr^{-1}$)	Distance (kpc)	Diameter (pc)	Reference[a]
G4.5+6.8.....	Kepler's SNR	3.2×10^{-19}	4.5	4	1
G13.3−1.3[b]		...	3.0	46	2
G18.8+0.3	Kes 67	2.7×10^{-20}	8.1	32	*
G31.9+0.0	3C 391	1.0×10^{-19}	7.2	12	3, 4
G33.6+0.1	Kes 79	3.3×10^{-20}	7.1	21	*
G43.3−0.2	W49B	4.8×10^{-19}	7.5	8	*
G46.8−0.3	HC 30	9.5×10^{-21}	6.4	28	*
G49.2−0.7	W51	2.7×10^{-20}	6.0	52	5
G53.6−2.2	3C 400.2	1.3×10^{-21}	5.0	44	*
G54.4−0.3	HC 40	2.6×10^{-21}	3.3	38	*
G74.0−8.5	Cygnus Loop	8.6×10^{-22}	0.8	45	6
G78.2+2.1	γ Cygni	1.4×10^{-20}	1.2	21	7, 8
G84.2−0.8		5.2×10^{-21}	4.5	24	9
G89.0+4.7	HB 21	3.1×10^{-21}	0.8	24	10
G111.7−2.1	Cas A	1.6×10^{-17}	3.4	5	11
G116.5+1.1		3.4×10^{-22}	5.0	101	*
G116.9+0.2	CTB 1	1.2×10^{-21}	3.1	31	12
G119.5+10.2.....	CTA 1	6.7×10^{-22}	1.4	37	13
G120.1+1.4	Tycho's SNR	1.3×10^{-19}	4.5	11	14
G132.7+1.3	HB 3	1.1×10^{-21}	2.2	51	15, 16
G156.2+5.7		6.2×10^{-23}	3.0	96	17, 18
G160.9+2.6	HB 9	9.9×10^{-22}	2.2	83	*
G166.0+4.3	VRO 42.05.01	5.5×10^{-22}	4.5	57	19
G166.2+2.5	OA 184	2.6×10^{-22}	4.5	104	19
G189.1+3.0	IC 443	1.2×10^{-20}	1.5	20	20
G205.5+0.5	Monoceros	5.0×10^{-22}	1.6	102	21
G260.4−3.4	Pup A	6.5×10^{-21}	2.2	35	22
G296.5+10.0.....	PKS 1209-52	1.2×10^{-21}	1.6	36	23, *
G304.6+0.1	Kes 17	3.3×10^{-20}	7.9	18	*
G309.8+0.0		5.4×10^{-21}	3.6	23	7
G315.4−2.3	RCW 86	4.2×10^{-21}	2.8	34	24
G327.6+14.6.....	SN 1006	3.2×10^{-21}	2.1	18	25, 26
G330.0+15.0.....	Lupus Loop	1.6×10^{-21}	1.2	63	27
G332.4−0.4	RCW 103	4.2×10^{-20}	3.4	10	*
G348.5+0.1	CTB 37A	4.8×10^{-20}	9.0	39	*
G348.7+0.3	CTB 37B	1.4×10^{-20}	9.0	45	*
G349.7+0.2		6.0×10^{-19}	13.8	9	*
G359.1−0.5		3.7×10^{-21}	9.2	64	28

Case & Battacharya, ApJ 504, 761, 1998

Σ-D relation (1)

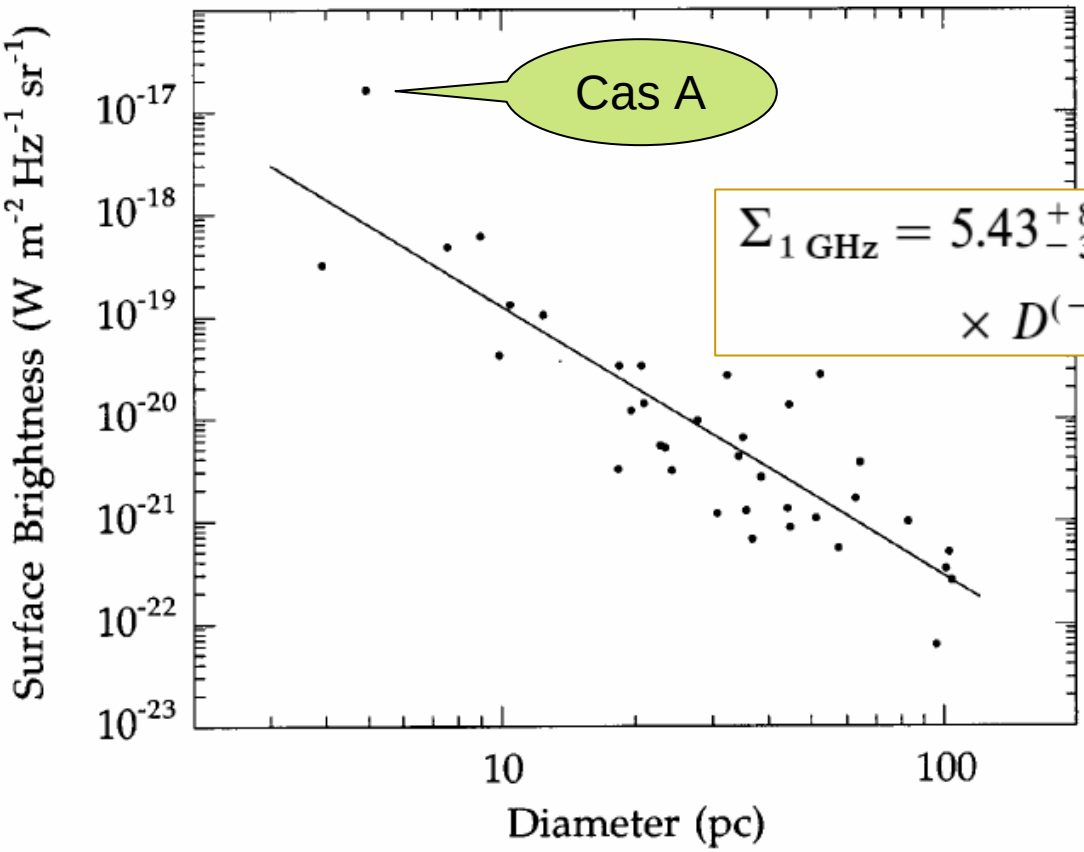

$$\Sigma_{1\,\mathrm{GHz}} = 5.43^{+8.16}_{-3.26} \times 10^{-17} \times D^{(-2.64 \pm 0.26)}\ \mathrm{W\ m^{-2}\ Hz^{-1}\ sr^{-1}}$$

FIG. 1.—The surface brightness vs. diameter (Σ-*D*) relation for shell SNRs using the distance calibrators in Table 1 (including Cas A).

Case & Battacharya, ApJ 504, 761, 1998

Σ-D relation (2)

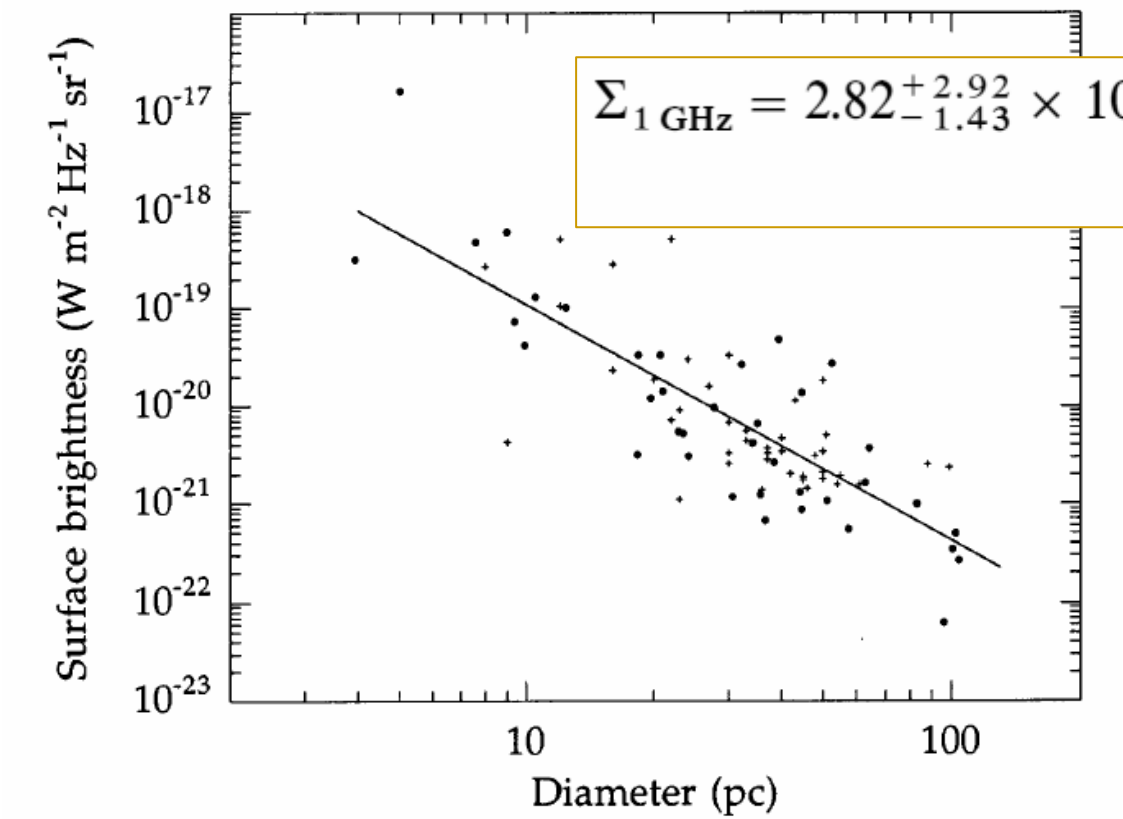

$$\Sigma_{1\,\mathrm{GHz}} = 2.82^{+2.92}_{-1.43} \times 10^{-17} D^{(-2.41 \pm 0.20)}$$

W m^{-2} Hz^{-1} sr^{-1}

With LMC + SMC samples

FIG. 4.—Σ-*D* relation (eq. [5]) for the Galactic (*filled circles*) and LMC + SMC (*crosses*) shell SNRs. This fit includes 78 remnants and does not differ significantly from that with the Galactic SNRs alone (eq. [3]).

Case & Battacharya, ApJ 504, 761, 1998

Surface brightness distribution

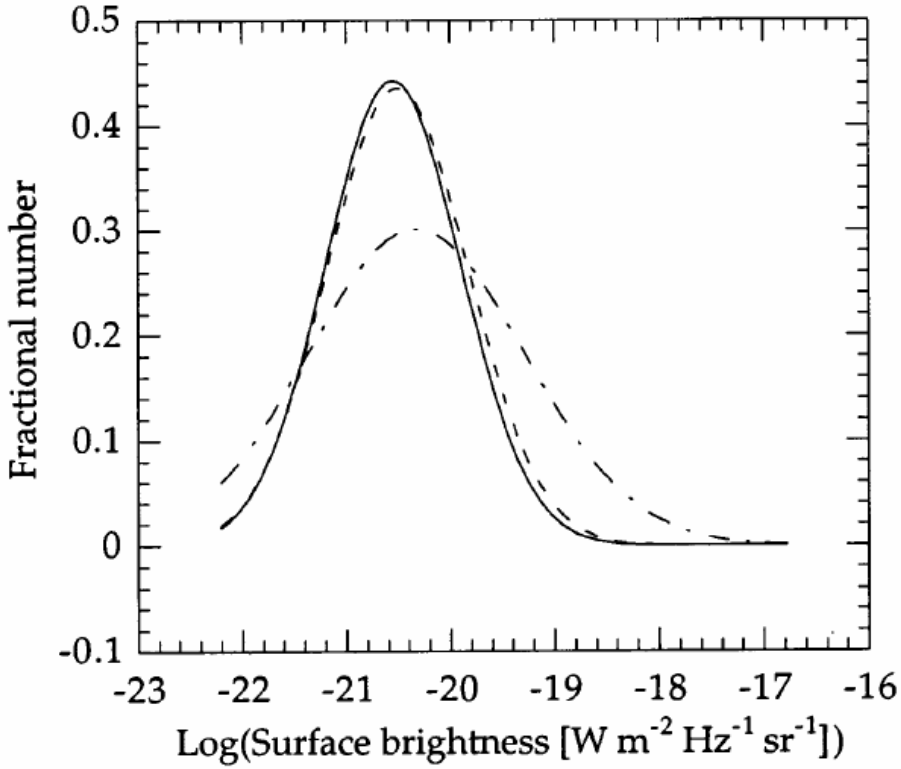

FIG. 2.—The surface brightness distributions for all shell SNRs in Green's catalog (*solid line*), the 20 shell SNRs within 3 kpc of the Sun (*dashed line*), and the sample of 36 shell SNRs (excluding Cas A) with known distances (*dot-dashed line*). The sample with known distances is biased toward brighter remnants. The distributions are fit to Gaussians with a lower cutoff at $\Sigma_c = 5 \times 10^{-23}$ W m^{-2} Hz^{-1} sr^{-1}. The distribution for shell SNRs within 3 kpc of the Sun is used to determine scale factors to compensate for observational selection effects (see § 4).

Case & Battacharya, ApJ 504, 761, 1998

Fractional error of distance

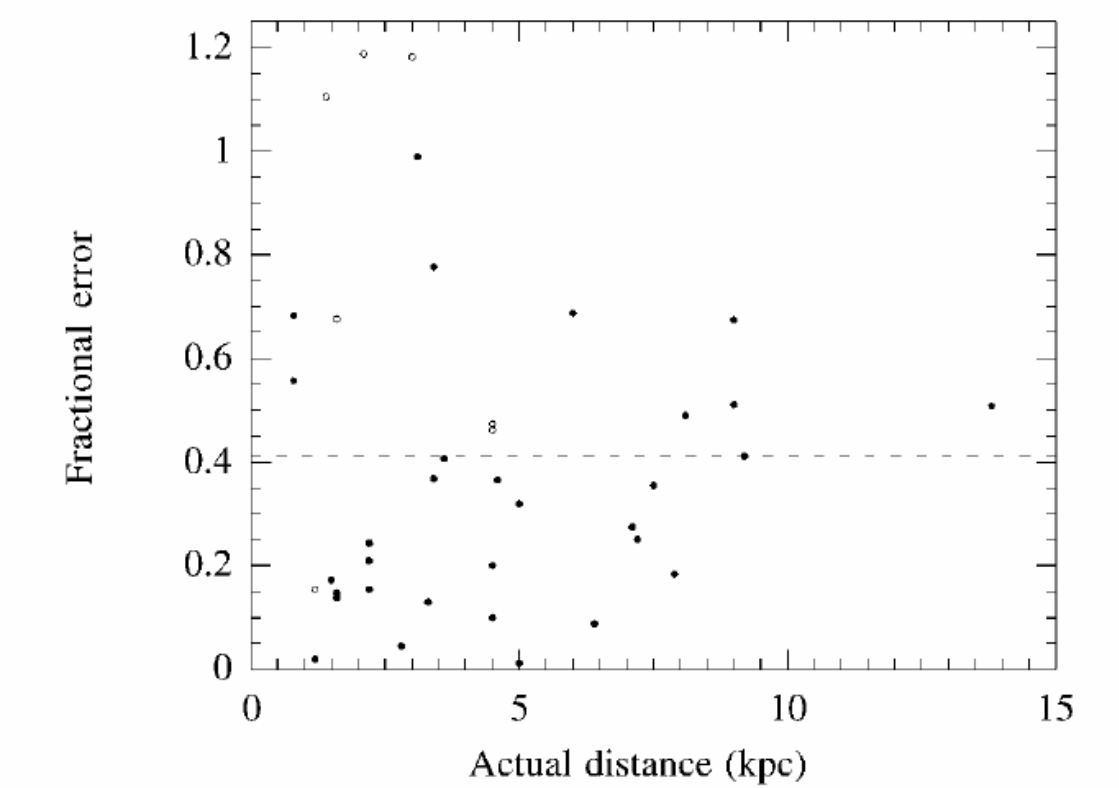

FIG. 3.—The fractional error, f, of the distances derived from our Σ-D relation with respect to the actual distances for the shell SNRs given in Table 1, excluding Cas A. The open circles are those shell remnants with $z > 200$ pc. The average fractional error for all of the remnants is 0.41 and is shown by the dashed line.

Case & Battacharya, ApJ 504, 761, 1998

Galactic SNR distribution

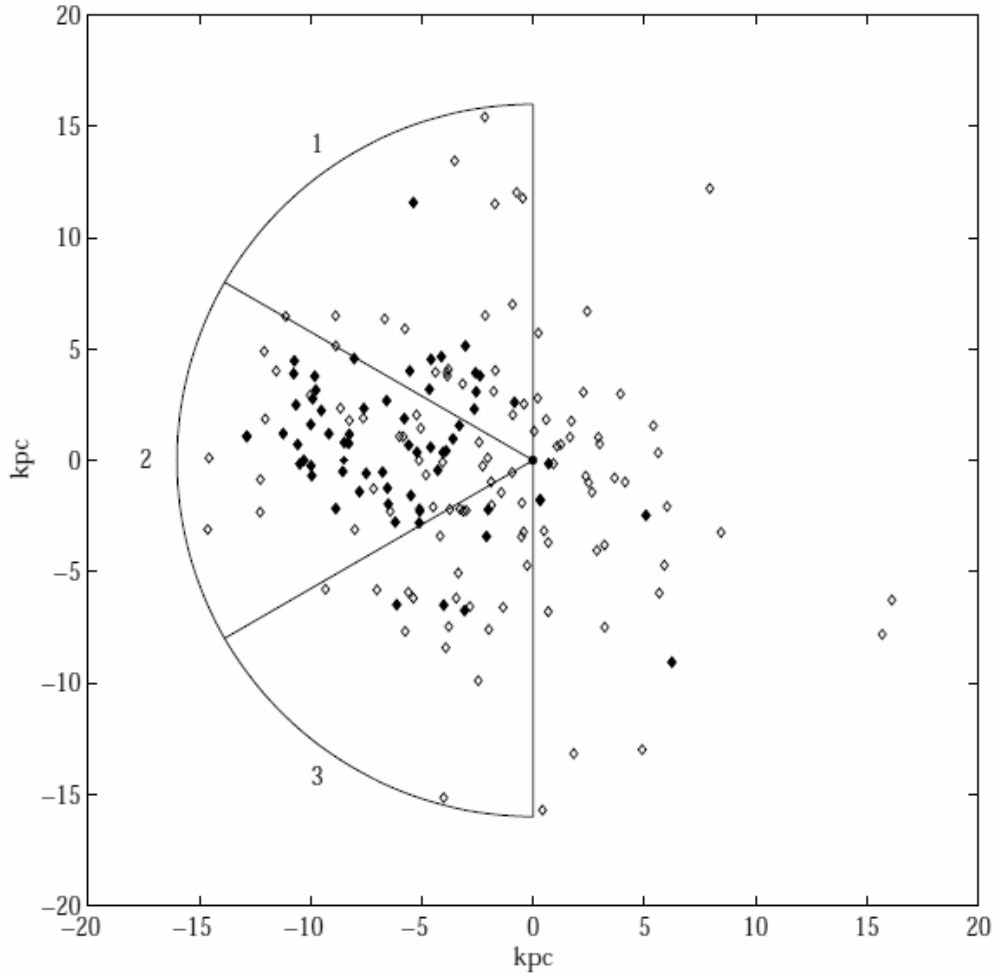

FIG. 6.—The Galactic SNR distribution using corrected distances and our new Σ-*D* relation. Filled-center and composite SNRs with known distances are included. Shell SNRs with distances derived from our Σ-*D* relation (see Table 3) are shown as open diamonds, while SNRs with known distances are shown as filled diamonds. The filled circle marks the Galactic center, and the asterisk marks the position of the Sun. Also shown are the three regions into which the near half of the Galaxy is divided (see § 4).

Case & Battacharya, A&AS 120, 437, 1996

Radial distribution

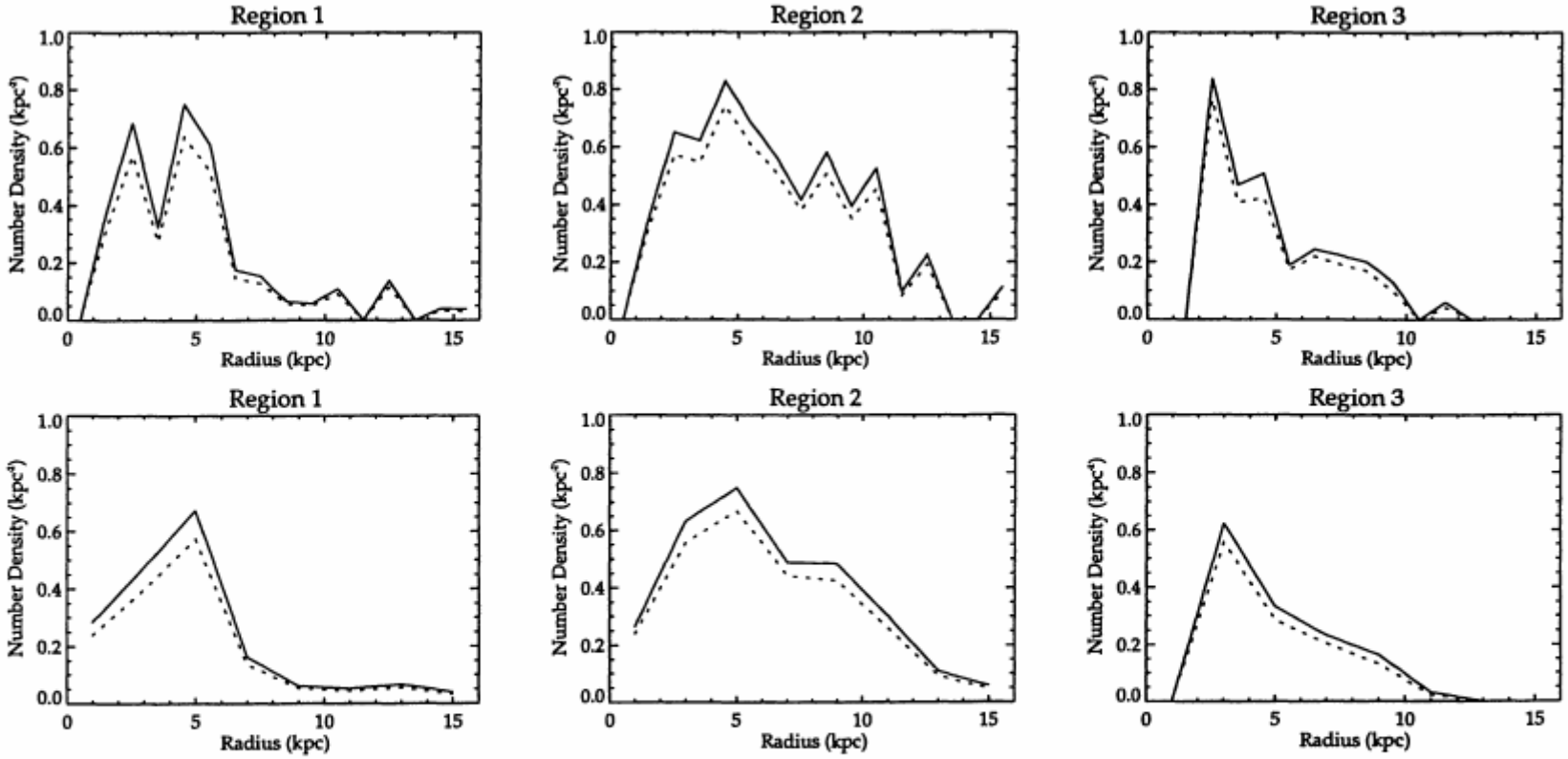

Fig. 2. The Supernova remnant density distribution as a function of radius for the three regions of the Galaxy described in the text. The solid line is the corrected density and the dotted line is the uncorrected density. The approximate positions of the spiral arms are apparent in the top three plots where 1 kpc radial bins were used. 2 kpc bins are used in the lower three plots and show the smooth distribution used for fitting

Case & Battacharya, A&AS 120, 437, 1996

Radial distribution function (1)

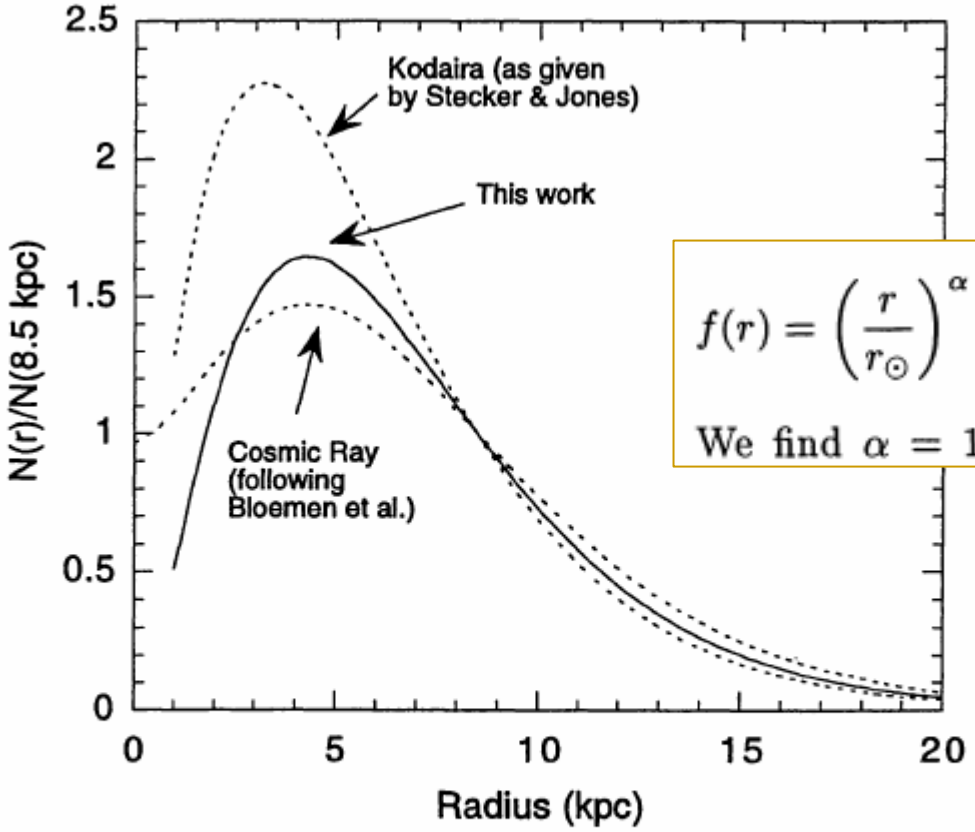

$$f(r) = \left(\frac{r}{r_\odot}\right)^{\alpha} \exp\left(-\beta \frac{r - r_\odot}{r_\odot}\right)$$

We find $\alpha = 1.69 \pm 0.22$ and $\beta = 3.33 \pm 0.37$;

Fig. 3. The functional form of the SNR density distribution and the resulting cosmic ray distribution are shown. All curves are normalized to 8.5 kpc

Case & Battacharya, ApJ 504, 761, 1998

Radial distribution function (2)

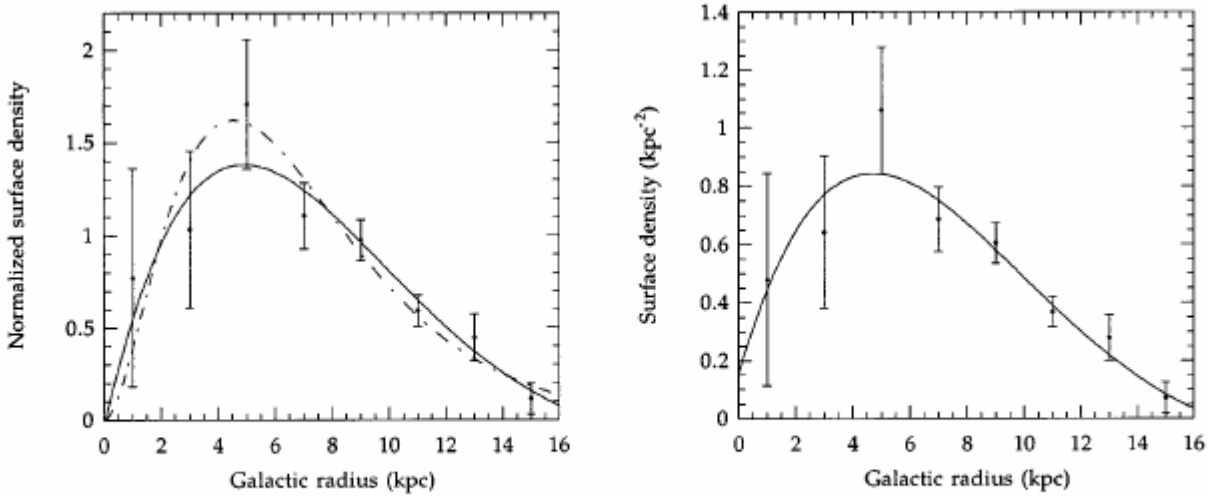

FIG. 7.—The SNR density radial distribution for region 2 using the new distances and compensation for selection effects. (*a*) The distribution derived in this work (*solid line and data points*) and that of Kodaira (1974) (*dashed line*), both normalized to the density at the radius of the solar circle. (*b*) The unnormalized data points and the fit to eq. (15).

$$f(r) = \left(\frac{r}{r_\odot}\right)^{\alpha} \exp\left(-\beta \frac{r - r_\odot}{r_\odot}\right)$$

$\alpha = 2.00 \pm 0.67$ and $\beta = 3.53 \pm 0.77$

$$f(r) = A \sin\left(\frac{\pi r}{r_0} + \theta_0\right) e^{-\beta r}$$

where $A = 1.96 \pm 1.38$ kpc^{-2}, $r_0 = 17.2 \pm 1.9$ kpc, $\theta_0 = 0.08 \pm 0.33$, and $\beta = 0.13 \pm 0.08$ kpc^{-1}. This fit is valid for $r < r_0(1 - \theta_0/\pi)$, i.e., 16.8 kpc; $f(r) = 0$ beyond that.

Total number of SNRs (<16kpc, $\Sigma > 5\times10^{-23}$Wm^{-2}Hz^{-1}sr^{-1}) ~ $336/f_z$ (f_z: completeness factor, 0.85-0.99)

Urosevic et al., AA 435, 437, 2005

SNRs in nearby galaxies

Table 1. General properties of the nearby galaxies with radio SNRs.

Galaxy	Hubble type[†]	Major and minor (arcmin)[†]	Distance (Mpc)	Incl. angle (degrees)[‡]	Number of radio SNRs
LMC	SB(s)m	645 × 550	0.055[a]	35	52
SMC	SB(s)m pec	320 × 185	0.065[a]	61	12
M 31	SA(s)b	190 × 60	0.75[b]	78	30
M 33	SA(s)cd	70.8 × 41.7	0.82[b]	56	53
IC 1613	IB(s)m	16.2 × 14.5	0.69[b]	27	1
NGC 300	SA(s)d	21.9 × 15.5	2.1[c]	46	17
NGC 6946	SAB(rs)cd	11.5 × 9.8	5.1[d]	42	35
NGC 7793	SA(s)d	9.3 × 6.3	3.38[e]	50	7
M 82	I0	11.2 × 4.3	3.9[f]	66	50
NGC 1569	IBm	3.6 × 1.8	2.2[g]	64	3
NGC 2146	SB(s)ab pec	6.0 × 3.4	14.5[h]	36	3

Note: [†]NED Database; [‡]Tully (1988); [a]Filipović (2002); [b]Freedman et al. (2001); [c]Freedman et al. (1992); [d]de Vaucouleurs (1979); [e]Puche & Carignan (1988); [f]Sakai & Madore (1999); [g]Israel (1988); [h]Tarchi et al. (2000).

...data sets made up of extragalactic SNRs do not suffer from Malmquist bias because all SNRs are at the same distance and are therefore sampled from the same volume. ...they do suffer from other selection effects from limitations in sensitivity and resolution, as well as from source confusion.

Urosevic et al., AA 435, 437, 2005

SNR surveys in nearby galaxies

Table 2. Resolution and sensitivity for searches for radio SNRs in nearby galaxies.

Galaxy	ν (GHz)	Resolution (arcsec)	Resolution (pc)	rms noise (μJy/beam)	Limiting L_ν ($\times 10^{22}$ $\frac{\text{erg}}{\text{s Hz}}$)	Reference
LMC	1.40	912	243	30 000	11	Filipović et al. (1998b)
SMC	1.42	828	261	15 000	7.7	Filipović et al. (1998b)
IC 1613	1.46	5	17	56	3.2	Lozinskaya et al. (1998)
M 31	1.465	5	18	30	2.0	Braun & Walterbos (199
M 33	1.42	7	28	50	4.1	Gordon et al. (1999)
NGC 300	1.45	4	39	60	30	Pannuti et al. (2000)
NGC 6946	1.45	2	49	20	63	Lacey et al. (1997)
NGC 7793	1.47	7	115	60	83	Pannuti et al. (2002)
M 82	8.4	0.182	3	360	660	Huang et al. (1994)
NGC 1569	1.412	0.20	2	25	15	Greve et al. (2002)
NGC 2146	1.6	0.17	12	35	890	Tarchi et al. (2000)

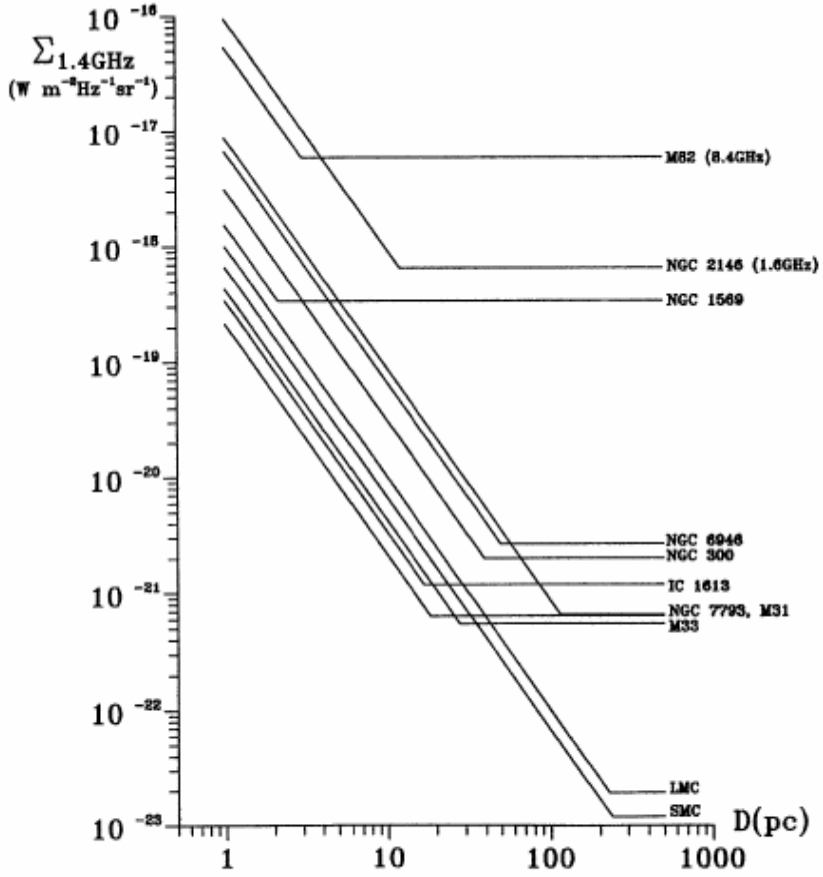

Fig. 3. Sensitivity lines in the $\Sigma - D$ plane for radio surveys of 11 nearby galaxies at 1.4 GHz. The sensitivity lines for M 82 and NGC 2146 are at 8.4 GHz and 1.6 GHz, respectively.

Urosevic et al., AA 435, 437, 2005

Σ-D relation in nearby galaxies (1)

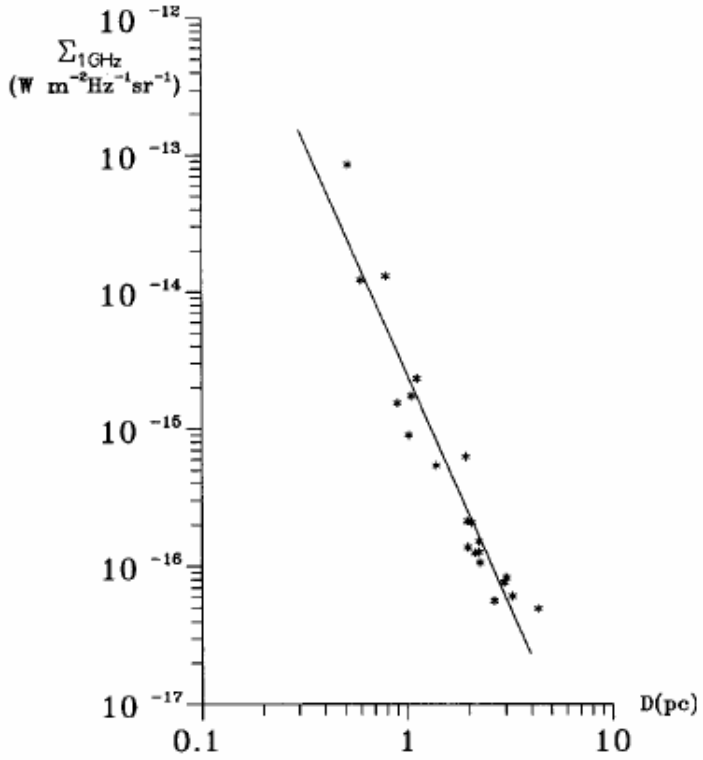

Fig. 1. The Σ – *D* diagram at a frequency of 1 GHz for 21 M 82 calibrators.

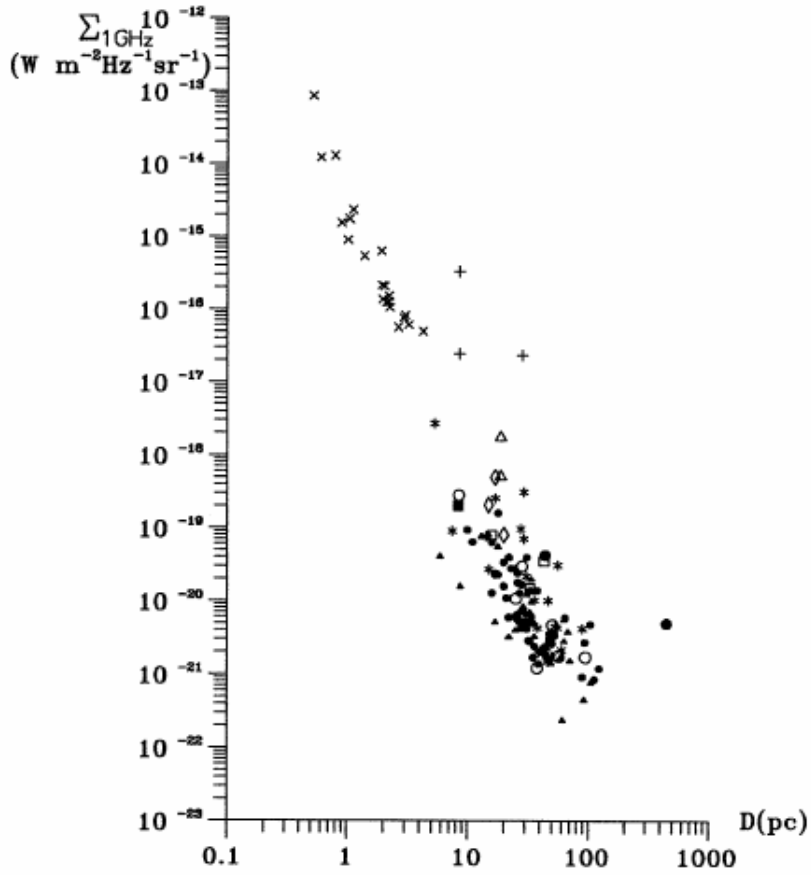

Fig. 2. The Σ – *D* diagram at a frequency of 1 GHz. The SNRs are represented by: asterisks (LMC), open circles (SMC), filled triangles (M 31), filled dots (M 33), open box (IC 1613), open squares (NGC 300), filled circles (NGC 7793), open triangles (NGC 6946), "x"'s (M 82), crosses (NGC 2146) and open diamonds (NGC 1569).

Urosevic et al., AA 435, 437, 2005

Σ-D relation in nearby galaxies (2)

Table 3. Fit characteristics of $\Sigma - D$ relations at 1 GHz for SNRs in nearby galaxies.

Galaxy	β (c.c.; f.q.)	No. of SNRs (comments)
M 31	1.67 ± 0.26 (–0.77; 60%)	30
M 33	1.77 ± 0.20 (–0.79; 62%)	51
LMC	2.28 ± 0.40 (–0.77; 59%)	25
SMC	2.28 ± 0.52 (–0.89; 80%)	7
Galactic (C&B)	2.38 ± 0.26 (–0.84; 71%)	36 (excluding Cas A)
M 82	3.41 ± 0.24 (–0.95; 91%)	21
"Master"		
	3.20 ± 0.11 (–0.92; 84%)	148 (complete sample)
	3.30 ± 0.09 (–0.95; 89%)	145 (excluding 3 HNRs)

Note: c.c. and f.q. represent the correlation coefficient and the fit quality, respectively.

Brogan et al., astro-ph/060145

35 New SNRs discovered by VLA

- VLA (90cm), 2002-2004
- ℓ=4.5° -22°, $|b|$<1.25°
- Resolved(>42”), spectrum α<0, bright IR

$S \propto \nu^{\alpha}$

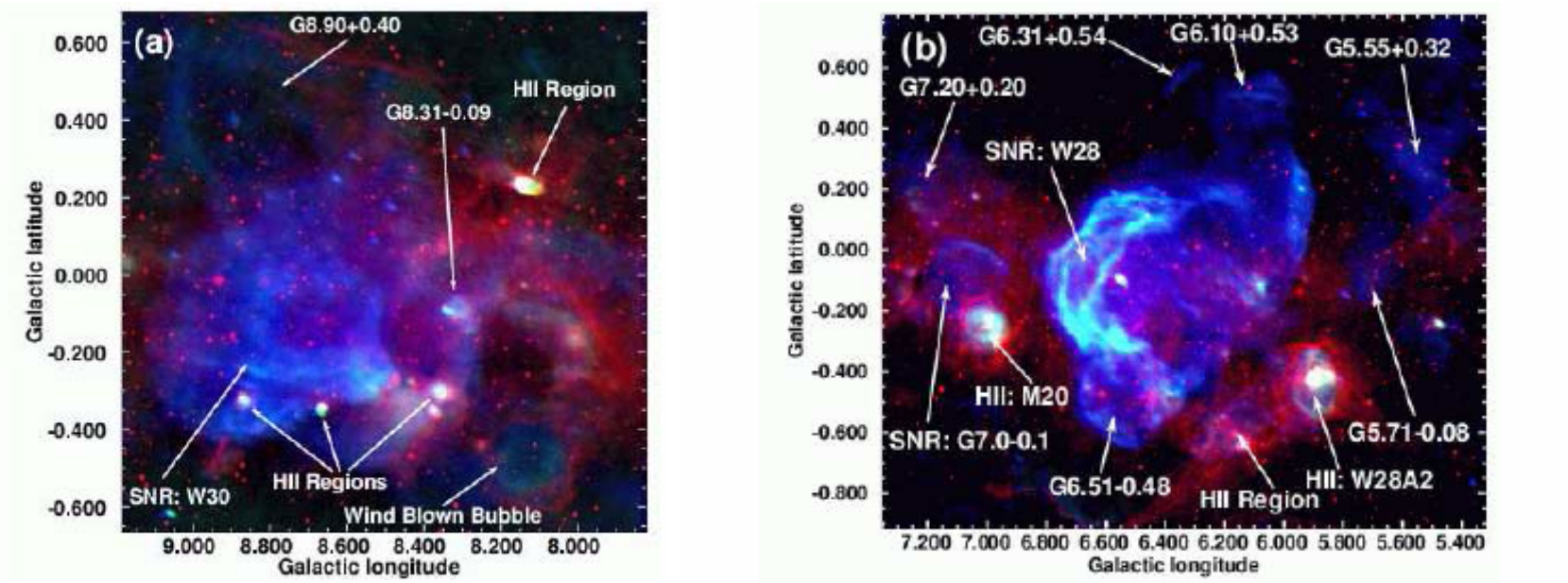

FIG. 1.— Three color images with *blue*=VLA 90cm, *red*=MSX 8 μm, and *green*=SGPS+VLA 20cm of the (a) W30 region and (b) W28 region. New SNRs are indicated using Galactic coordinates; the previously known SNRs, H II regions, and a WBB are also labeled.

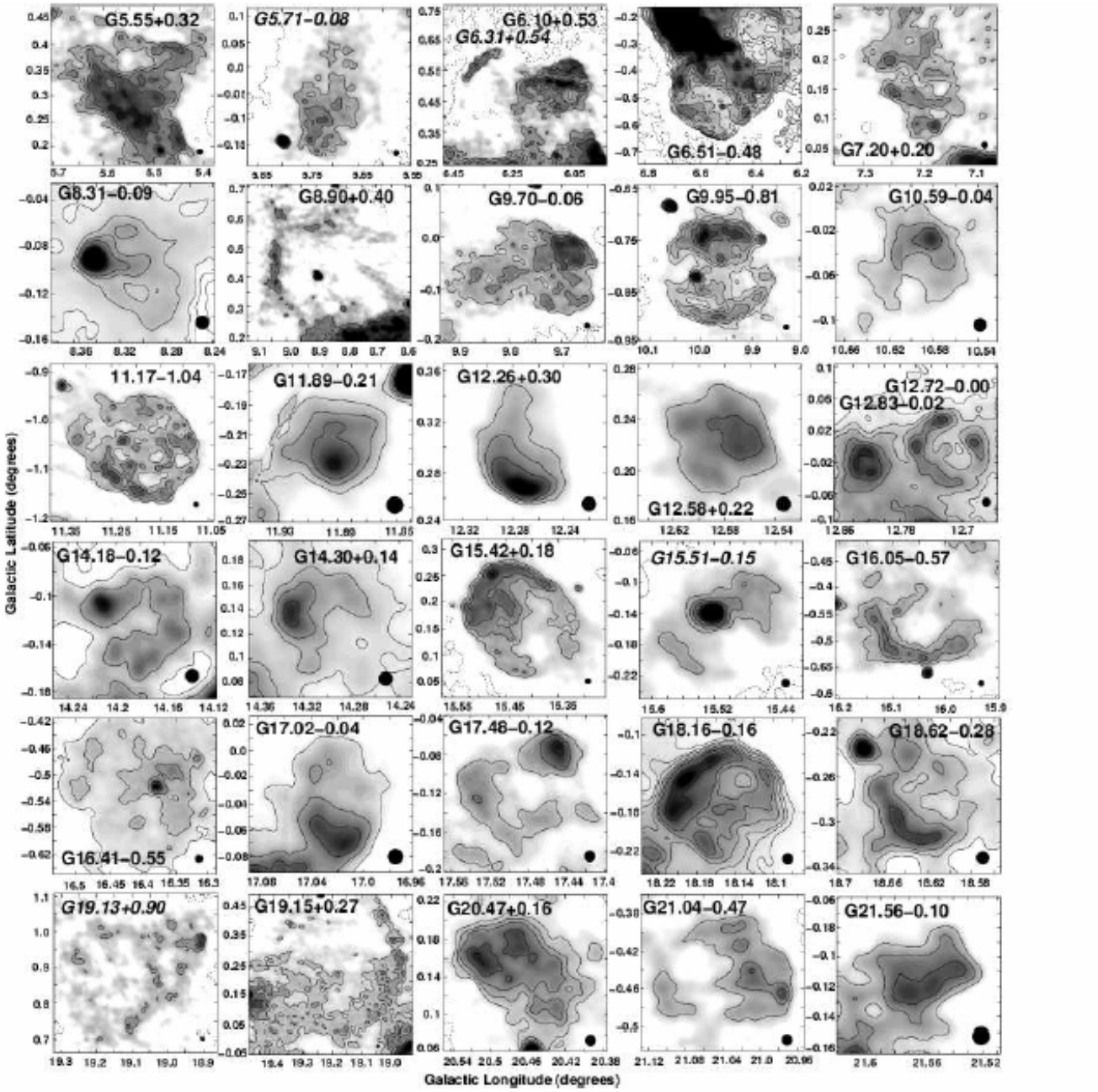

FIG. 2.— VLA 90cm images of the newly discovered SNRs (excluding three shown in Brogan et al. (2004)). The contour levels on each image are -25, 25, 37.5, 50, 75, 100, & 125 mJy beam^{-1}. For latitudes $|b| \lesssim 0.5°$, 25 mJy beam^{-1} is approximately 5σ, while it is $\sim 3\sigma$ at higher latitudes. The resolution of these images is 42″; the beam size is shown in the lower right of each panel for comparison. Class III sources are labeled in italics.

TABLE 1
PROPERTIES OF SNR CANDIDATES

ℓ (°)	b (°)	R. A. (h m s)	Dec. (° ′)	Size (′ x ′)	Morphology[a]	Class	S_{90cm}[b] (Jy)	S_{20cm}[b] (Jy)	S_{11cm}[b] (Jy)	$\alpha_{(90/20)}$[c]	$\alpha_{(90/11)}$[c]	Notes[d]
5.55	+0.32	17 57 04	−24 00	12 x 15	Shell	II	14.3 (0.3)	4.6 (0.9)	3.9 (0.4)	−0.8	−0.6	
5.71	−0.08	17 58 49	−24 03	9 x 12	Partial Shell	III	4.3 (0.2)	2.0 (0.6)	1.6 (0.2)	−0.5	−0.5	
6.10	+0.53	17 57 29	−23 25	18 x 12	Partial Shell	I	13.4 (0.2)	3.5 (0.7)	2.0 (0.2)	−0.9	−0.9	
6.31	+0.54	17 57 54	−23 14	3 x 9	Filament	III	1.4 (0.1)	0.7 (0.3)	0.3 (0.1)	−0.5	−0.8	
6.51	−0.48	18 02 11	−23 34	18 x 18	Shell	I	60.8 (0.4)	22.1 (1.1)	22.7 (2.3)	−0.7	−0.5	H/O
7.20	+0.20	18 01 07	−22 38	12 x 12	Partial Shell	II	5.2 (0.2)	2.3 (0.7)	1.8 (0.2)	−0.6	−0.5	H
8.31	−0.09	18 04 34	−21 49	5 x 4	Shell	II	2.3 (0.1)	1.0 (0.2)	0.5 (0.1)	−0.6	−0.7	H
8.90	+0.40	18 03 58	−21 03	24 x 24	Shell	II	18.2 (0.5)	...	4.9 (0.5)	...	−0.6	
9.70	−0.06	18 07 22	−20 35	15 x 11	Shell	I	6.5 (0.2)	3.0 (0.7)	1.5 (0.2)	−0.5	−0.7	H
9.95	−0.81	18 10 41	−20 43	12 x 12	Shell	II	11.0 (0.3)	5.9 (0.8)	4.6 (0.5)	−0.4	−0.4	
10.59	−0.04	18 09 08	−19 47	6 x 6	Partial Shell	II	1.4 (0.1)	0.7 (0.3)	0.3 (0.1)	−0.5	−0.7	X
11.03	−0.05	18 10 04	−19 25	9 x 11	Partial Shell	I	3.1 (0.2)	1.1 (0.5)	1.0 (0.1)	−0.7	−0.5	O/X
11.15	−0.71	18 12 46	−19 38	11 x 7	Partial Shell	I	2.3 (0.1)	0.8 (0.4)	0.4 (0.1)	−0.7	−0.8	H/O
11.17	−1.04	18 14 03	−19 46	18 x 12	Shell	I	11.0 (0.3)	4.7 (0.8)	4.1 (0.4)	−0.6	−0.5	O
11.18	+0.11	18 09 47	−19 12	12 x 10	Shell	I	3.5 (0.2)	2.0 (0.5)	1.6 (0.2)	−0.4	−0.4	H/O
11.89	−0.21	18 12 25	−18 44	4 x 4	Shell	II	0.9 (0.1)	0.6 (0.2)	0.4 (0.1)	−0.3	−0.4	H/X
12.26	+0.30	18 11 17	−18 10	5 x 6	Partial Shell	I	1.5 (0.1)	0.6 (0.3)	0.4 (0.1)	−0.7	−0.6	H
12.58	+0.22	18 12 14	−17 55	5 x 6	Composite?	II	0.8 (0.1)	0.5 (0.3)	0.3 (0.1)	−0.4	−0.5	
12.72	−0.00	18 13 19	−17 54	6 x 6	Shell	I	2.0 (0.1)	0.6 (0.3)	0.3 (0.1)	−0.8	−0.8	H
12.83	−0.02	18 13 37	−17 49	3 x 3	Shell	I	1.2 (0.1)	0.7 (0.2)	0.4 (0.1)	−0.4	−0.5	H/O/X
14.18	−0.12	18 15 52	−16 34	6 x 5	Shell	II	0.9 (0.1)	0.4 (0.3)	0.3 (0.1)	−0.6	−0.5	
14.30	+0.14	18 15 58	−16 27	5 x 4	Partial Shell	II	1.2 (0.1)	0.5 (0.3)	0.6 (0.1)	−0.5	−0.3	
15.42	+0.18	18 18 02	−15 27	14 x 15	Shell	I	10.9 (0.3)	4.6 (0.8)	2.9 (0.3)	−0.6	−0.6	
15.51	−0.15	18 19 25	−15 32	8 x 9	Shell	III	4.2 (0.2)	1.9 (0.5)	1.0 (0.1)	−0.5	−0.7	
16.05	−0.57	18 21 56	−15 14	15 x 10	Shell	I	4.9 (0.2)	2.2 (0.7)	1.3 (0.1)	−0.6	−0.6	
16.41	−0.55	18 22 38	−14 55	13 x 13	Partial Shell	II	10.0 (0.3)	3.6 (0.9)	2.0 (0.2)	−0.7	−0.8	
17.02	−0.04	18 21 57	−14 08	5 x 5	Shell	I	0.7 (0.1)	0.4 (0.3)	0.3 (0.1)	−0.5	−0.4	H
17.48	−0.12	18 23 08	−13 46	6 x 6	Partial Shell	II	0.9 (0.1)	0.3 (0.4)	0.3 (0.1)	−0.7	−0.6	
18.16	−0.16	18 24 34	−13 11	8 x 8	Shell	I	7.6 (0.1)	3.9 (0.4)	3.0 (0.3)	−0.5	−0.4	H/O/X
18.62	−0.28	18 25 55	−12 50	6 x 6	Partial Shell	II	1.9 (0.1)	1.2 (0.4)	0.7 (0.1)	−0.3	−0.5	H
19.13	+0.90	18 22 37	−11 50	24 x 18	Partial Shell	III	27.2 (0.5)	...	9.4 (0.9)	...	−0.5	
19.15	+0.27	18 24 56	−12 07	27 x 27	Partial Shell	II	17.4 (0.4)	...	5.5 (0.6)	...	−0.5	
20.47	+0.16	18 27 51	−11 00	8 x 8	Shell	I	4.2 (0.1)	2.7 (0.4)	1.4 (0.1)	−0.3	−0.5	H
21.04	−0.47	18 31 12	−10 47	9 x 7	Shell	II	2.3 (0.2)	0.9 (0.5)	0.5 (0.1)	−0.6	−0.7	
21.56	−0.10	18 30 50	−10 09	5 x 5	Partial Shell	II	0.5 (0.1)	0.3 (0.2)	0.2 (0.1)	−0.4	−0.6	H/X

[a] "Partial shell" morphology indicates that $\lesssim$ 70% of a complete shell is evident in the 90cm image.

[b] Statistical uncertainties are provided in parenthesis, for the 90 and 21cm data they are calculated from (# independent beams)$^{0.5} \times 3\sigma$, while it is the larger of 10σ or 10% for the 11cm data.

[c] Spectral indices between indicated wavelengths using $S_\nu \propto \nu^\alpha$; the uncertainty in α is typically the larger of $|\ \alpha(90/20) - \alpha(90/11)\ |$ or 0.2.

[d] H: also candidate in Helfand et al. (2005b). O: previously reported in (ascending ℓ order) Yusef-Zadeh et al. (2000); Brogan et al. (2004); Brogan et al. (2004); Trushkin (1996); Brogan et al. (2004); both Brogan et al. (2005) and Helfand et al. (2005a); Odegard (1986). X: Possible *ASCA* X-ray counterpart in Sugizaki et al. (2001) or Bamba et al. (2003).

Distribution on the Galactic plane

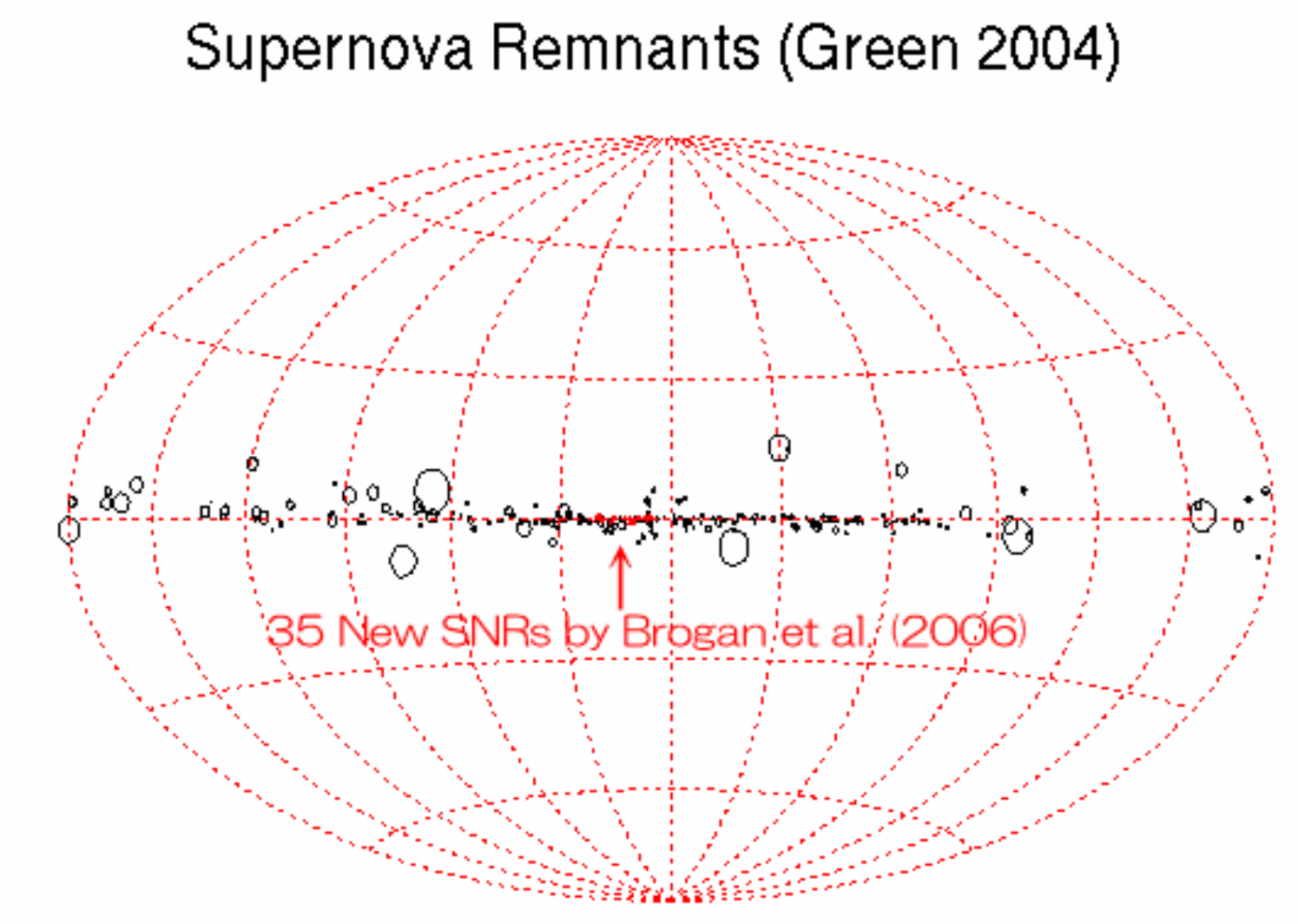

Longitudinal distribution

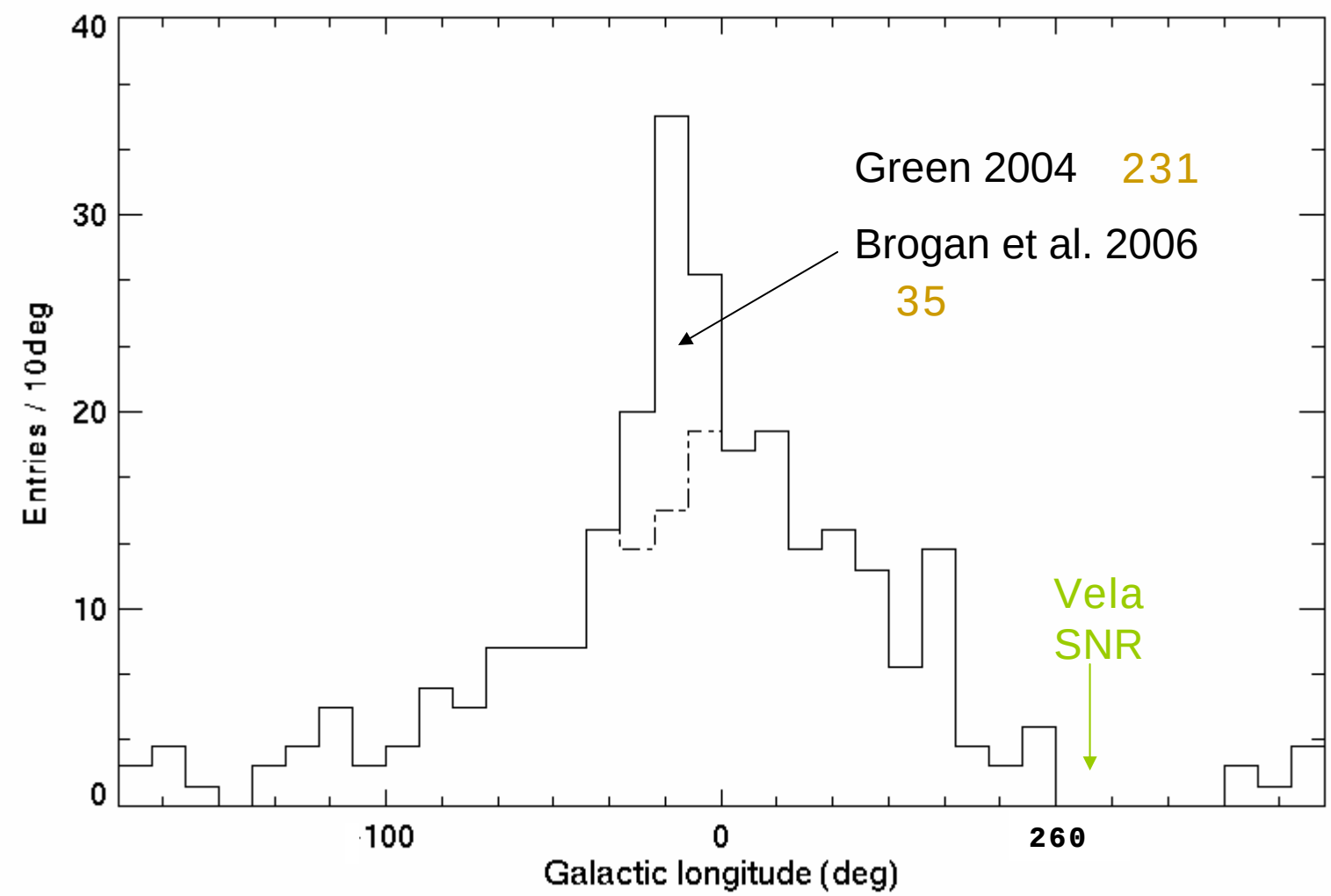

Evolution of SNRs

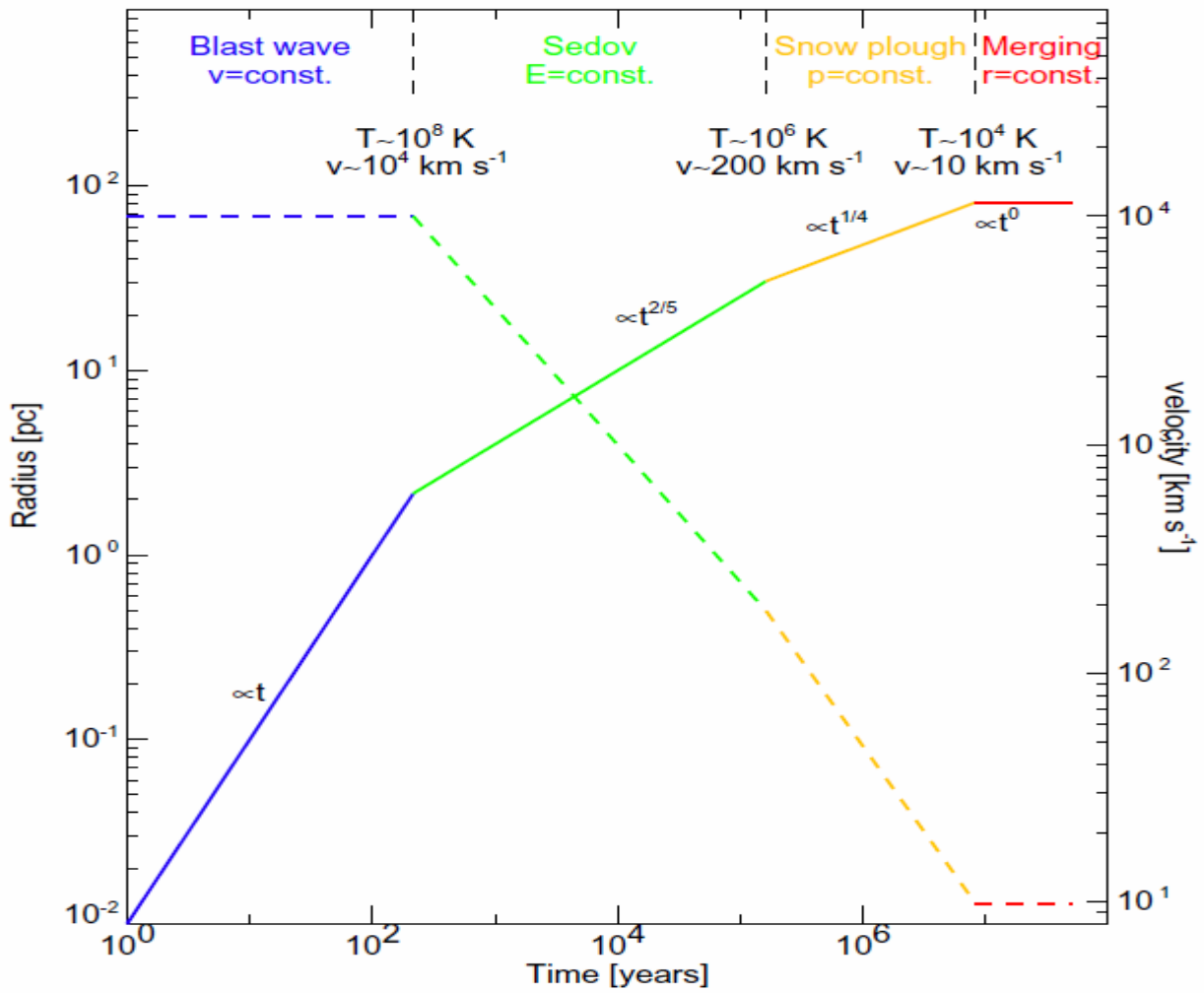

after Padmanabhan (2002, Fig. 4.6)

CR energetics & SNR: How many TeV SNRs?

- Number of active SNRs in Galaxy
  - SN rate ~ 1/30yr, accelerating particles during ~ 10^4yr
    $\Rightarrow$ ~300 active SNRs
    $\Rightarrow$ ~3 SNRs within 1kpc (assuming Case & Battacharya distribution [A&AS 120, 437,1996])
- We have two SNRs (RXJ1713, RXJ0852) emitting ~1*Crab* TeV gamma-rays, both at ~1 kpc
  - L_γ ~ 6×10^{35}erg/s (>GeV, assuming $E^{-2.6}dE$)
  - 300 SNRs $\Rightarrow$ W_γ(Galaxy) ~ 2×10^{38}erg/s
- Cosmic ray power in Galaxy
  - 1 eV/cm^3, V~$10^{66\text{-}67}$cm^3, τ~$10^{14\text{-}15}$s $\Rightarrow$ W_{CR} ~10^{40}erg/s
- $\therefore$ $W_\gamma \sim 0.02 W_{CR}$: low efficiency!? Or more SNRs?